Premodified Surface Method to Obtain Ultra-highly Dispersed Metals and their 3D Structure Control on an Oxide Single-crystal Surface

Satoru Takakusagi*[a], Yasuhiro Iwasawa[b] and Kiyotaka Asakura[a]

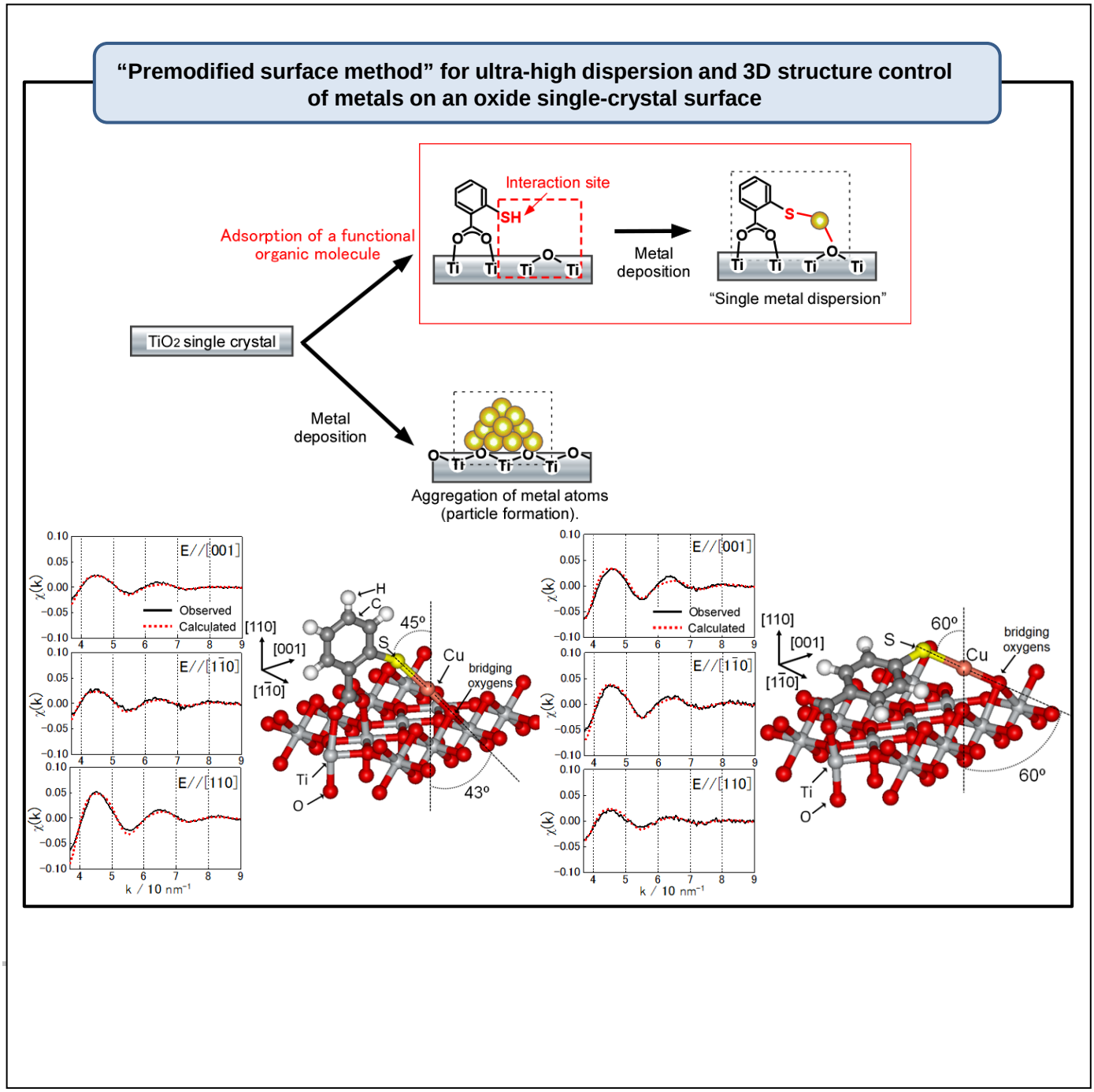

Abstract: Precise control of the three-dimensional (3D) structure of highly dispersed metal species such as metal complexes and clusters attached to an oxide surface has been important for the development of next-generation high-performance heterogeneous catalysts. However, this is not easily achieved for the following reasons. (1) Metal species are easily aggregated on an oxide surface, which makes it difficult to control their size and orientation definitely. (2) Determination of the 3D structure of the metal species on an oxide powder surface is hardly possible. To overcome these difficulties, we have developed the premodified surface method, where prior to metal deposition, the oxide surface is premodified with a functional organic molecule that can strongly coordinate to a metal atom. This method has successfully provided a single metal dispersion on an oxide single-crystal surface with the 3D structure precisely determined by polarization-dependent total reflection fluorescence X-ray absorption fine structure (PTRF-XAFS). Here we describe our recent results on ultra-high dispersions of various metal atoms on TiO_2(110) surfaces premodified with mercapto compounds, and show the possibility of fine tuning and orientation control of the surface metal 3D structures.

1. Introduction

Catalysts are one of the key materials for the development of a sustainable society and play a critical role in the industrial production of various chemicals. Over 80% of catalytic processes use heterogeneous catalysts to achieve high conversion and/or selectivity through lowering the activation barriers to lead to the desired products.[1,2] The majority of these materials consist of active transition metal species that are highly dispersed on oxide supports, such as SiO_2, Al_2O_3, TiO_2, MgO, or CeO_2. Well-defined metal species such as metal complexes and clusters that exhibit high catalytic performance can be attached by grafting organometallic compounds on an oxide surface through reaction with OH groups or by anchoring the metal species via a linker molecule that interacts with both the metal and the oxide support.[3-5] The local structures and oxidation states of the resultant surface metal species can be monitored using several characterization techniques. X-ray absorption fine structure (XAFS) is one of the most powerful techniques to detect atomic-level structure and the oxidation state of deposited metal species. Transmission electron microscopy (TEM) is also widely used to obtain information on the size and local structure of such metal species. However, the species are typically immobilized on an oxide powder surface, so that it is difficult to determine their three-dimensional (3D) structure with respect to the oxide support surface to understand and optimize the synergistic interaction between the metal and support. Therefore, it is necessary to use a single-crystal surface as an oxide support for 3D structure detection of the metal species. Polarization-dependent total reflection fluorescence X-ray absorption fine structure (PTRF-XAFS) analysis can provide 3D structural information regarding highly dispersed metal species on an oxide single-crystal surface due to the high surface sensitivity of this technique.[6,7] Our group has previously determined the 3D structures of Cu, Co, Pt, and Mo complexes, and their derivatives grafted onto SiO_2(0001), Al_2O_3(0001), and TiO_2(110) with the aim of elucidating the metal-support interactions at the atomic level.[8-13]

Grafting metal species on an oxide surface typically requires the preparation of organometallic compounds in advance, even though they are often unstable and readily decompose in contact with air or at elevated temperatures, thereby causing significant aggregation on the oxide surface. In contrast, if the oxide support surface is premodified using an organic ligand that strongly anchors metal atoms to the surface through covalent bonds, then attachment of ultra-highly dispersed metal species such as monatomic metal species can be expected without the need for organometallic compounds. We have successfully prepared atomically dispersed metals (single metal dispersion) with this technique on the basis of metal-ligand bonding, simply by vacuum deposition of metal atoms onto an oxide single-crystal surface premodified with a functional organic molecule (Figure 1), and their 3D structures were precisely determined using the PTRF-XAFS technique.[14-17] For example, when *ortho*-mercaptobenzoic acid (*o*-MBA) is used as the premodification molecule, monatomic Cu, Au and Ni atoms are energetically stabilized on the TiO_2(110) surface by the formation of bonds with sulfur of the adsorbed *o*-MBA and the bridging oxygen in the TiO_2 lattice, whereas aggregation of the metal atoms occurs easily in the absence of *o*-MBA. In this system, the carboxylic acid group of the MBA acts to bind the compound to the TiO_2 substrate. We refer to this technique as the premodified surface method, and various organic compounds may be available for the purpose of surface premodification. Fine tuning and orientation control of metal species on an oxide surface are also important to modify the metal-support interaction, which has a significant effect on their catalytic properties and electron transfer processes from the metal (support) to the support (metal). MBA has three isomers, *o*-, *m*- and *p*-MBA, which have different mercapto group distances from the surface, where the S atom position is expected to influence the local structure and orientation of the metal species.

(Insert Figure 1 here.)

Figure 1. Surface premodification by a functional organic molecule to obtain an ultra-highly dispersed metal (single metal dispersion) on an oxide single-crystal surface.

It should be noted that these monatomic metal species prepared by the premodified surface method can be used as building blocks to construct well-controlled metal nanoparticle structures, such as dimers, trimers, tetramers, and small clusters

[a] Dr. S.Takakusagi and Prof. K. Asakura
Institute for Catalysis
Hokkaido University
N21W10, Kita-ku, Sapporo, Hokkaido, Japan
E-mail: takakus@cat.hokudai.ac.jp
[b] Prof. Y. Iwasawa
Innovation Research Center for Fuel Cells and Graduate School of Informatics and Engineering
The University of Electro-Communications
1-5-1 Chofugaoka, Chofu, Tokyo, Japan

(<1 nm). These species should exhibit unique catalytic properties depending on the number of atoms.[18-22]

Here, we first describe the principles of the PTRF-XAFS technique briefly in Section 2, which is a unique method to determine the 3D structures of highly dispersed metal species on oxide single-crystal surfaces. In Section 3, we review our recent PTRF-XAFS results on the dispersion behaviors of Cu, Au, Ni and Pt atoms on TiO_2(110) premodified with *o*-MBA. Based on the 3D structure characterization of various metal species on the *o*-MBA-modified TiO_2(110) surface by PTRF-XAFS, we discuss the basic factors that govern surface metal dispersion and propose an indicator to obtain a single metal dispersion. We also show the possibility of fine tuning and orientation control of the surface metal 3D structures in Section 4, including their coordination and configuration against the surface according to the different mercapto group positions of the three MBA isomers (*o*-, *m*-, and *p*-MBA). Finally in Section 5, we summarize our results and describe future developments for the precise control of 3D structures and the reactivity of metals on oxide surfaces by the premodified surface method.

Satoru Takakusagi was born in 1975 in Gunma, Japan. He received his Bachelor's, Master's and Ph.D. degrees from the University of Tokyo in 1998, 2000 and 2003, respectively, under the supervision of Prof. Yasuhiro Iwasawa. He became an Assistant Professor at Faculty of Science, Hokkaido University in 2002 and was promoted to Associate Professor of Institute for Catalysis (ICAT), Hokkaido University in 2008. He received the Chemical Society of Japan (CSJ) Presentation Award 2008, Young Investigator Encouragement Award by CSJ Hokkaido Branch in 2014, and Hokkaido University President's Award for Excellence in Research (AY 2014). His current research interests focus on atomic-level structure and reactivity of well-defined model catalyst surfaces.

Yasuhiro Iwasawa was born in 1946 in Saitama, Japan. He received his Ph.D. degree from The University of Tokyo in 1973. He became Professor at Department of Chemistry, The University of Tokyo in 1986. He moved to the University of Electro-Communications in Tokyo as Professor due to retirement at the University of Tokyo in 2009. He was President of the Chemical Society of Japan in 2010–2012. He also served as Head of Science and Technology Section of Science Council of Japan, Cabinet Office in 2008–2011. He is President of the Chemical Society Union, Japan. His honors include National Medal with Purple Ribbon from Emperor and Prime Minister (2003), The Chemical Society of Japan Award (2004), etc. His current research interests are in in-situ/operando characterization and chemical design of catalysts and surfaces on the molecular level involving fuel cells.

Kiyotaka Asakura was born in 1958 in Fukuoka, Japan. He received his Ph.D. degree from the University of Tokyo in 1987. He joined Prof. Yasuhiro Iwasawa group as a research associate in Department of Chemistry, the University of Tokyo in 1984. He became an associate professor of Research Center for Spectrochemistry, the University of Tokyo in 1994. Since 1999 he has been a full professor of Institute for Catalysis, Hokkaido University. He served as Director of Institute for Catalysis in 2015-2018. He has authored over 300 scientific publications and received the Young Scientist Award from the Catalysis Society of Japan in 1993, Surface Science Society of Japan and Catalysis Society of Japan awards in 2014 and 2015. He is now on the editorial board of several international journals such as the PCCP, Topics in Catalysis and Catalysis Letters. His current research interests are in the development of new methods related to catalyst and surface science.

2. PTRF-XAFS technique for 3D structure determination

XAFS is a powerful technique to obtain local structure information such as bond distance and coordination number around an X-ray absorbing atom with sub-angstrom resolution. XAFS does not require long range crystalline order; therefore, the structures of oxide-supported metal catalysts where metal species are highly dispersed on powdery oxides have been extensively studied. The structural information derived from XAFS is averaged over all spatial directions, so that it is difficult to determine accurate 3D and interface structures of the dispersed metals species. However, if XAFS can be applied to such metal species on an oxide single-crystal surface as a model catalyst surface, then we could obtain more fruitful and definite information regarding the 3D structure of supported metal species and the metal-support interaction. For example, the XAFS oscillation $\chi(k)$ at K and L_1 edges has the $\cos^2\theta_i$ dependence on the angle θ_i between the electric vector ($\vec{E}$) of the incident X-rays and the bond R_i as shown in Figure 2(a). Thus, the measurement of polarization-dependent XAFS (Figure 2(b)) can provide information on the corresponding 3D structure. The fluorescence detection method is used, which provides a high-sensitivity XAFS signal for the dilute metal species at single-crystal surfaces as small as 10^{13} cm^{-2}. Grazing incidence X-ray alignment is also applied so that the incident X-rays make a total reflection and cannot penetrate into the bulk (penetration depth is only a few nanometers) to enhance the surface sensitivity of X-rays and reduce the background signals from the bulk. This technique is thus called polarization-dependent total reflection fluorescence X-ray absorption fine structure (PTRF-XAFS).[6,7]

(Insert Figure 2 here.)

Figure 2. (a) Polarization dependence of XAFS oscillation $\chi(k)$. $\chi_i(k)$ is the XAFS oscillation originated from the bond R_i. (b) PTRF-XAFS measurements by sample rotation.

The other surface science techniques which can provide the 3D structure around the specific metal adatom on an oxide single-crystal surface are X-ray standing wave (XSW)[23-25] and photoelectron diffraction (PD) including photoelectron holography.[26-28] XSW allows one to determine the location of adatom sites relative to the underlying bulk crystal in an X-ray standing wave caused by the interference of the incident and scattered X-ray beams at a Bragg reflection though it cannot directly give the bond distances between an adatom and its neighboring atoms. On the other hand, PD and PTRF-XAFS can give direct information on bond distance and bond direction based on the coherent interference of the photoelectron wavefield directly emitted from an adatom and elastically scattered by the surrounding atoms.[27] And PTRF-XAFS has an advantage over PD when one wants to follow the 3D structure of the catalytically active metal adatom in the presence of reactant gases because PTRF-XAFS is a photon-in photon-out technique though PD requires a vacuum environment for photoelectron detection.

3. Ultra-high dispersion of metals on TiO_2(110) premodified with *o*-MBA

Various metal atoms (Cu, Au, Ni and Pt) are vacuum-deposited on TiO_2(110) premodified with *o*-MBA to examine its effects on the dispersion of the metal atoms over the surface. The carboxylic acid group of *o*-MBA binds to TiO_2(110) with the bridge-bidentate form (Figure 3(b)),[29] and the adsorbed *o*-MBA molecules form a densely packed monolayer according to spectroscopic ellipsometry and X-ray photoelectron spectroscopy (XPS) measurements.[15,17] Homogeneity of the deposited metal species was checked by the width and shape of the corresponding photoelectron peaks (Cu2p, Au4f, Ni2p and Pt4f) in the XPS measurements. Coverages of the metal atoms were also determined from the XPS results, where 1 monolayer (ML) was defined as the density of surface 5-fold coordinated Ti (Ti_{5c}) atoms in Figure 3(a) (5.2×10^{14} cm^{-2}). Considering the anisotropic surface structure of TiO_2(110) as shown in Figure 3(a), PTRF-XAFS measurements were conducted employing three different orientations relative to the electric vector ($\vec{E}$) of the incident-X-rays: ($\vec{E}$//[$\mathbf{001}$], [$\mathbf{1\bar{1}0}$] and[$\mathbf{110}$]).

(Insert Figure 3 here.)

Figure 3. (a) Structure model of the TiO_2(110) surface. (b) Adsorbed structure of *o*-MBA on TiO_2(110). Reprinted with permission from Ref. 17. Copyright (2016) American Chemical Society.

3.1. Cu/*o*-MBA/TiO_2(110)

Figure 4 shows the PTRF-XAFS spectra for Cu on the *o*-MBA-modified TiO_2(110) surface (Cu/*o*-MBA/TiO_2(110)), in addition to spectra for reference compounds.[15] The Cu coverage was 0.42 ML. The envelopes of the PTRF-XAFS oscillations in Figure 4(a) were quickly damped in the higher *k* region, compared to that for Cu foil. This indicated that the nearest neighbor atom of Cu was not Cu, but a lighter atom such as sulfur or oxygen. The polarization dependence was such that the amplitudes of the XAFS oscillations in the [001] and [$1\bar{1}0$] directions were almost equal, and were smaller than that in the [110] direction. Presence of such polarization dependence in the PTRF-XAFS spectra indicates that the Cu bonds are not randomly oriented but oriented to specific directions, suggesting formation of uniform metal species. The curve fitting analysis indicated no contribution from Cu-Cu interaction, which suggested that no Cu aggregation occurred. Cu-S (0.219±0.003 nm) and Cu-O (0.185±0.003 nm) interactions were dominant in the three observed spectra. Previous results for Cu deposited directly on a TiO_2(110) surface revealed that Cu was easily aggregated to form particles, even at a very low coverage of 0.03 ML.[30] It was therefore concluded that Cu aggregation was effectively blocked on the surface by the presence of sulfur atoms in the coadsorbed *o*-MBA molecules.

(Insert Figure 4 here.)

Figure 4. (a) Cu K-edge PTRF-XAFS spectra of Cu/*o*-MBA/TiO_2(110). (b) Cu K-edge XAFS spectra of reference compounds. Reproduced from Ref. [15] with permission of The Royal Society of Chemistry.

To determine the accurate 3D structure of the Cu species, an iteration method was employed using a FEFF code and a real-space model structure.[31] Figures 5(a) and (b) show the polarization-dependent FEFF simulation and the proposed model structure, respectively. The EXAFS oscillations calculated from the model were in good agreement with the observed spectra. The Cu–S and Cu–O bond angles to the surface normal were 45° and 43°, respectively, where the precision by FEFF simulation was less than 3°. The S–Cu–O bond angle was estimated to be 177°, which was close to 180°. ($\vec{E}$//[001], [$1\bar{1}0$] and[110]).

(Insert Figure 5 here.)

Figure 5. (a) Observed (black solid lines) and calculated (red dotted lines) PTRF-XAFS spectra for Cu/*o*-MBA/TiO_2(110), respectively. The 3D model structure shown in (b) was used to calculate the theoretical $\chi(k)$ in (a). Reproduced from Ref. [15] with permission of The Royal Society of Chemistry.

It has been previously reported that the stable adsorption sites for Cu on a bare TiO_2(110) surface could be atop sites of the bridging oxygens, because a bridging oxygen has a dangling bond pointing upwards from the surface.[32] However, Cu deposited directly on a bare TiO_2(110) surface was aggregated to form clusters.[30] This indicated that the strength of the Cu-bridging oxygen bond was not sufficient to fix the Cu atom. The Cu atom could thus easily migrate to other atop sites of bridging oxygen atoms until it reached a Cu island, which resulted in aggregation to form Cu metal clusters. In contrast, the S atom of *o*-MBA preadsorbed on the TiO_2(110) surface could immediately

catch and immobilize the migrating Cu atom in cooperation with the bridging oxygen, accompanied by the rotation of the bond connecting the COO- moiety and phenyl ring. The formation reaction of the S-Cu-O bonding motif can be described as follows.

o-MBA_{ad} + Cu + 2O (bridging) → *o*-MBA_{ad}-Cu-O (bridging) + HO (bridging) (1)

3.2. Au/*o*-MBA/TiO_2(110)

The interaction of Au with the TiO_2 surface is rather weak and it is reported that even at a small coverage (ca. 0.03 ML) Au was easily aggregated to form small clusters on a TiO_2(110) surface.[33]

In the curve fitting analysis of the PTRF-XAFS spectra for Au/*o*-MBA/TiO_2(110) (Au coverage: 0.1 ML), no contribution from Au-Au interaction was detected, whereas Au-S (0.232±0.003 nm) and Au-O (0.210±0.003 nm) interactions were dominant in all three orientations ($\vec{E}$//[001], [1$\bar{1}$0] and[110]).[16] Figure 6 shows the 3D model structure obtained by the FEFF simulation. Au atoms were also sandwiched by the sulfur of *o*-MBA_{ad} and the bridging oxygen in the TiO_2 lattice, similar to the arrangement revealed for Cu/*o*-MBA/TiO_2(110). The Au–S and Au–O bond angles to the surface normal were 59° and 37°, respectively, where the precision by FEFF simulation was less than 4°. The S–Au–O bond angle was 156°, which was slightly smaller than the S–Cu–O angle (177°). This is probably because the metal-S and metal-O bond distances were longer in the Au system than those in the Cu system due to the different atomic sizes.

(Insert Figure 6 here.)

Figure 6. 3D model structure for Au/*o*-MBA/TiO_2(110). Reproduced from Ref. [16] with permission of The Royal Society of Chemistry.

3.3. Ni/*o*-MBA/TiO_2(110)

The interaction of Ni with the TiO_2 surface is much stronger than that of other meals such as Cu and Au. Previous studies of Ni deposited directly on a TiO_2(110) surface showed that atomically dispersed Ni was stabilized only at specific step edges (<11$\bar{n}$>) through the formation of two Ni-O bonds (O-Ni-O), and that the Ni atoms were located at imaginary Ti sites when the Ni coverage was very low (ca. 0.02 ML).[34] Aggregation of Ni was also observed with the formation of clusters on the terrace surfaces when the coverage was increased above 0.05 ML.[35,36]

However, in the analysis of the PTRF-XAFS spectra for Ni/*o*-MBA/TiO_2(110), the *o*-MBA-modified TiO_2(110) surface stabilized the atomically dispersed Ni species, even at 0.27 ML coverage because no contribution from Ni-Ni interaction was evident, while Ni-S (0.219±0.003 nm) and Ni-O (0.185±0.003 nm) interactions were dominant.[17] The FEFF simulation gave the model structure shown in Figure 7 for the Ni/*o*-MBA/TiO_2(110) system. Ni formed a similar local structure to those for Cu and Au, which was the S-metal-O bonding motif. The Ni–S and Ni–O bond angles relative to the surface normal were 57° and 40°, respectively, and the precision of the FEFF simulation was better than 3°. The S–Ni–O bond angle was estimated to be 156°. The bond distances for meta-S and metal-O in the Ni and Cu systems were similar, but the corresponding S-metal-O angles were different, which may be due to the different form of coordination between Ni and Cu atoms

(Insert Figure 7 here.)

Figure 7. 3D model structure for Ni/*o*-MBA/TiO_2(110). Reprinted with permission from Ref. 17. Copyright (2016) American Chemical Society.

In the same manner as Cu, Ni atoms could not be stabilized on the terrace surfaces by bond formation between Ni and a bridging oxygen[37] so that the Ni atoms hopped to the next bridging oxygen and diffused along the [001] direction. The Ni atoms eventually found other Ni atoms and formed clusters before reaching the step edges when the Ni coverage was sufficiently high (>0.05 ML). In the present study, a TiO_2(110) surface with a very low step density (less than 4 lines every 1 μm^2) was used and the number of Ni atoms stabilized at specific step edges (<11$\bar{n}$>) would thus be negligible. The S atoms of *o*-MBA adsorbed on the TiO_2(110) terrace surfaces could immediately immobilize the migrating Ni atoms in cooperation with the bridging oxygens. Thus, Ni aggregation was effectively blocked on the surface, even at a high Ni coverage (0.27 ML).

3.4. Pt/*o*-MBA/TiO_2(110)

Figure 8 shows the PTRF-XAFS spectra for Pt on the *o*-MBA-modified TiO_2(110) surface (Pt/*o*-MBA/TiO_2(110), Pt coverage: 0.11ML), in addition to spectra for reference compounds.[17] In Figure 8(a), no significant degree of polarization-dependence was observed. In addition, curve fitting analysis shown in Table 1 demonstrated the presence of Pt-S (0.229 nm) and Pt-Pt (0.267 nm) bonds in all the three orientations, which suggested aggregation of the Pt atoms. Considering that the effective coordination number (N*) of the Pt-Pt bond was around 2, the average Pt structure could be a trimer species. However, it is also possible that a mixture of atomically dispersed Pt and small Pt clusters, such as dimers, trimers, and tetramers, were formed on the surface.

(Insert Figure 8 here.)

Figure 8. (a) Pt L_3-edge PTRF-XAFS spectra of Pt/*o*-MBA/TiO_2(110). (b) Pt L_3-edge XAFS spectra of reference compounds. Reprinted with permission from Ref. 17. Copyright (2016) American Chemical Society.

(Insert Table 1 here.)

Table 1. Curve fitting results for Pt/*o*-MBA/TiO_2(110) data obtained at three different polarization directions.[a] *N**, *r*, ΔE, σ are the effective coordination number, bond distance, energy shift in the origin of the photoelectron kinetic energy and Debye-Waller factor, respectively. Reproduced with permission from Ref. 17. Copyright (2016) American Chemical Society.

A previous scanning tunneling microscopy (STM) study of Pt deposited on a bare TiO_2(110) surface revealed that Pt had aggregated to form clusters with heights below 0.8 nm, even at a low coverage of 0.07 ML.[38] From the detection of Pt-S bonds and the formation of small clusters at a Pt coverage of 0.11 ML, it was concluded that premodification of the TiO_2(110) surface with *o*-MBA effectively suppressed any significant aggregation of the deposited Pt atoms, although the dispersion effect of *o*-MBA was not sufficiently strong to produce a perfect atomic dispersion of Pt atoms.

3.5. Factors governing single metal dispersion on *o*-MBA/TiO_2(110)

As described in 3.1–3.4, monatomic metal atoms were stabilized for Cu, Au and Ni on the *o*-MBA-modified TiO_2(110) surface by the formation of bonds with the sulfur of *o*-MBA_{ad} and the bridging oxygen in the TiO_2 lattice, while Pt was aggregated to form small clusters at ca. 0.1 ML. In Table 2, the strengths of metal-metal (M-M) and metal-S (M-S) bonds (as assessed according to their bond dissociation energies at 298 K, D°_{298}) are listed for Cu, Au, Ni, and Pt.[39,40] The D°_{298}(M-M) value for Pt was the highest among the four metals, and Pt was the only metal for which D°_{298}(M-M) was greater than D°_{298}(M-S). These results indicate that metal-S bond formation is energetically more favorable than metal-metal bond formation in the case of Cu, Au and Ni, but not for Pt. This is in agreement with the Pt/*o*-MBA/TiO_2(110) results discussed in Section 3.4. The affinity of the metal atoms for oxygen would also be important in addition to the affinity for sulfur to account for the stability of the S-metal-O bond. Thus, the metal-oxygen (M-O) bond strengths (D°_{298}(M-O)) for Cu, Au, Ni, and Pt are also listed in Table 2.[33,35] The affinity for oxygen decreases in the order of Ni>Cu>Pt>Au. A term, R_{S-M-O}, which roughly estimates the formation preference and energetic stability of the S-metal-O bonding motif compared with metal-metal bond formation, was defined as follows.

$$R_{\mathrm{S-M-O}} = \frac{D^\circ_{298}(\mathrm{M-S}) + D^\circ_{298}(\mathrm{M-O})}{D^\circ_{298}(\mathrm{M-M})} \quad (2)$$

The $R_{\mathrm{S-M-O}}$ values for Cu, Au, Ni, and Pt were 3.1, 2.8, 3.6, and 1.6, respectively. The R_{S-M-O} value for Pt was the lowest, which indicates that this metal generates the least stable S-metal-O bonding motif. The aggregation of Pt was the most likely to proceed because it had the highest D°_{298}(M-M), lowest D°_{298}(M-S) and second-lowest D°_{298} (M-O) values, which indicates the preferential formation of Pt-Pt bonds and results in clustering on the *o*-MBA/TiO_2(110). In the case of Cu and Ni, both D°_{298}(M-S) and D°_{298} (M-O) values contribute almost equally to the corresponding $R_{\mathrm{S-M-O}}$ values. In contrast, for Au, the D°_{298}(M-S) value makes a much greater contribution than the D°_{298}(M-O) value. Although the D°_{298}(M-O) and D°_{298}(M-M) values for Au were the lowest and second-highest among the four metals, respectively, this metal had a relatively high $R_{\mathrm{S-M-O}}$ of 2.8 because of its high D°_{298}(M-S). These results suggest a high affinity of Au atoms for S atoms, which is in good agreement with previous reports.[42] R_{S-M-O} is thus a good indicator for metal atomic dispersion.

Table 2. Strengths of metal-metal (M-M), metal-sulfur (M-S), metal-oxygen (M-O) bonds (bond dissociation energies at 298 K, D°_{298}) for Cu, Au, Ni and Pt,[39] and the corresponding $R_{\mathrm{S-M-O}}$ values.

Metal	D°_{298}(M-M) / kJ/mol	D°_{298}(M-S) / kJ/mol	D°_{298}(M-O) / kJ/mol	$R_{\mathrm{S-M-O}}$	
Cu	177	276	269	3.1	O[b]
Au	226	418	221	2.8	O[c]
Ni	201	344	382	3.6	O[d]
Pt	307	233[a]	246[a]	1.6	X[d]

[a] D°_{298} (M-S) and D°_{298} (M-O) for Pt are taken from Refs. 40 and 41, respectively. [b] Ref. 15. [c] Ref. 16. [d] Ref. 17. O and X indicate single metal dispersion of the evaporated metal atoms and aggregation of them, respectively. Reproduced with permission from Ref. 17. Copyright (2016) American Chemical Society.

4. Fine tuning and orientation control by using different MBA isomers

The possibility of fine tuning and orientation control of the surface metal nanostructure was explored using different MBA isomers. Figure 9 shows the model structure for Cu/*m*-MBA/TiO_2(110) determined by FEFF simulation that reproduced the observed spectra well, where the local structure around Cu was similar to that in Cu/*o*-MBA/TiO_2(110) (Figure 5(b)).[15] The S-Cu-O bonds had an almost linear structure (angle = 176°) with the Cu–S and Cu-O bond distances at 0.219 nm and 0.185 nm, respectively. The Cu–S and Cu–O bond angles to the surface normal were 44° and 41°, respectively, where the precision by FEFF simulation was less than 4°. Note that one Ti-carboxylate bond of the adsorbed *m*-MBA had to be cleaved to give a monodentate adsorption structure so that Cu could form bonds with S and O atoms. This result indicates that formation of the linear S-Cu-O structure was energetically favored, even though one Ti-carboxylate bond in the adsorbed *m*-MBA was cleaved.

(Insert Figure 9 here.)

Figure 9. 3D model structure for Cu/*m*-MBA/TiO_2(110). Reproduced from Ref. [15] with permission of The Royal Society of Chemistry.

Figure 10(a) shows the PTRF-XAFS spectra for Cu/*p*-MBA/TiO_2(110).[15] The XAFS spectra showed a different polarization dependence from those for Cu/*o*-MBA/TiO_2(110) in

Figure 5(a), where the amplitude of XAFS oscillation in the [110] direction was smaller than that in the other two directions. The curve fitting analysis indicated Cu-S (0.223±0.004 nm) and Cu-O (0.190±0.003 nm) contributions to the observed spectra. Figures 10(a) and (b) show polarization-dependent FEFF simulation and the model structure for Cu/*p*-MBA/TiO_2(110), respectively. The Cu–S and Cu–O bond angles to the surface normal were both 60°, and the S–Cu–O bond angle was estimated to be 180°, where the precision by FEFF simulation was less than 4°. As expected, the Cu-S and Cu-O bonds were more parallel to the surface than those of Cu/*o*-MBA/TiO_2(110) and Cu/*m*-MBA/TiO_2(110), probably due to the limited conformation of adsorbed *p*-MBA to form a bond with Cu attached to a bridging oxygen through sulfur. The Cu-S and Cu-O bond distances were slightly longer than those for Cu/*o*-MBA/TiO_2(110) and Cu/*m*-MBA/TiO_2(110), which could also be due to distortion in the structure arising from the more flat-lying orientation of the Cu-S and Cu-O bonds formed by the Cu species compared with those for Cu/*o*-MBA/TiO_2(110) and Cu/*m*-MBA/TiO_2(110). One Ti-carboxylate bond of the adsorbed *p*-MBA was cleaved, and a monodentate adsorption structure was adopted, similar to that for Cu/*m*-MBA/TiO_2(110).

(Insert Figure 10 here.)

Figure 10. (a) Observed (black solid lines) and calculated (red dotted lines) PTRF-XAFS spectra for Cu/*p*-MBA/TiO_2(110). The 3D model structure shown in (b) was used to calculate the theoretical $\chi(k)$ in (a). Reproduced from Ref. [15] with permission of The Royal Society of Chemistry.

The results in this section clearly suggest the possibility of fine tuning and orientation control of surface metal nanostructures through the use of different MBA isomers. The difference in orientation may modify the synergistic effect of the oxide support on the metal species and would thus affect chemical reactivity of the metal species.

5. Summary and outlook

We have proposed the premodified surface method to obtain ultra-highly dispersed metal species on an oxide single-crystal surface, by which the oxide surface is premodified before metal deposition with a functional organic molecule that has a substituent atom that can strongly coordinate to the metal atom. Atomically dispersed metal species were successfully obtained for Cu, Au and Ni on a TiO_2(110) surface premodified with *o*-MBA by forming a similar local structure (S-metal-O bonding motif), and their 3D structures were precisely determined using the PTRF-XAFS technique. In contrast, Pt was aggregated to form small clusters due to the lower affinity of Pt atoms for S atoms than that of the other metal atoms. Thus, organic molecules with a functional group that has stronger interaction with Pt atoms than the mercapto-group would be indispensable to obtain single metal dispersion for Pt. R_{S-M-O} is a good indicator to suggest whether or not metal atoms are atomically dispersed on an oxide surface premodified with mercapto compounds.

We proposed the possibility to achieve fine tuning and orientation control of a metal species on an oxide surface through the use of different isomers as premodification molecules. The difference in orientation between Cu/*o*-MBA/TiO_2 and Cu/*p*-MBA/TiO_2 was clearly detected by PTRF-XAFS. Such structure modification leads to a new synergetic effect and chemical control by adjustment of the interaction between the oxide support and the metal species, which would affect the chemical reactivity of the metal.

One of the further important developments in the proposed system is to modify local geometric/electronic structures of atomically dispersed metal species through the use of premodified molecules that have different functional groups such as $–NH_2$, -COOH and –N≡C, and then to control the coordination environment around active metal sites. Another important development is a stepwise synthesis of mono- and multi-metallic clusters such as dimer, trimer, tetramer and small clusters (<1 nm) using such atomically dispersed metal species as building blocks. Metal deposition is performed by metal vapor deposition (MVD) in this study; therefore, it is possible to accurately control the amount of metal atoms deposited and prepare sub-nanoclusters on an oxide surface with one-atom precision. The size-dependent catalytic properties of small metal clusters, including single metal sites on an oxide surface, have attracted much attention recently because these metal species exhibit unique catalytic performance depending on the number of atoms.[18-22] Therefore, an atomic-level understanding of the 3D structure-activity relationship of these species is essential for optimization and further development, which is possible by combining the PTRF-XAFS technique and catalytic activity measurements.

Acknowledgements

The authors express their thanks to Prof. Wang-Jae Chun, Dr. Hiromitsu Uehara, Dr. Yuki Wakisaka, Dr. Hiroko A. Miwa, Dr. Takahiro Wada and Dr. Yohei Uemura for helpful technical support and fruitful discussions. This work was financially supported by a Grant-in-Aid for Scientific Research on Innovative Areas “Nano Informatics” (No. 25106010) and by a Grant-in-Aid for Scientific Research (B) (No. 18H01864) from the Japan Society for the Promotion of Science (JSPS). This research was also performed as a “PEFC project” (P10001) of the New Energy and Industrial Technology Development Organization (NEDO).

Keywords: Premodified surface method• Heterogeneous catalysts • Single meal dispersion • 3D structure • PTRF-XAFS

[1] G. Ertl, H. Knözinger, F. Schüth, J. Weitkamp, *Handbook of Heterogeneous Catalysis*, *2nd ed.*, *Vol.1*, Wiley–VCH, Weinheim, **2008**.

[2] G. A. Somorjai, Y. Li, *Introduction to surface chemistry and catalysis*, *2nd ed.*, Wiley, **2010**.

[3] a) Y. Iwasawa, *Catal. Today* **1993**, *18*, 21-72; b) M. Tada, Y. Iwasawa, *Chem. Commun.* **2006**, 2833-2844; c) M. Tada, Y. Iwasawa, *Coord. Chem. Rev*. **2007**, *251*, 2702-2716.

[4] a) C. Copéret, A. Comas-Vives, M. P. Conley, D. P. Estes, A. Fedorov, V. Mougel, H. Nagae, F. Núñez-Zarur, P. A. Zhizhko, *Chem. Rev.* **2016**,

116 , 323-421; b) C. Copéret, M. Chabanas, R. Petroff Saint-Arroman, J.-M. Basset, *Angew. Chem. Int. Ed.* **2003***, 42,* 156-181.

[5] a) M. Flytzani-Stephanopoulos, B.C. Gates, *Annu. Rev. Chem. Biomol. Eng.* **2012**, *3*, 545–574; b) A. Kulkarni, R.J. Lobo-Lapidus, B.C. Gates, *Chem. Commun.* **2010**, *46*, 5997–6015.

[6] K. Asakura in *Catalysis* (Eds.: J.J. Spivey and M. Gupta), RSC publishing, Cambridge, **2012**, pp. 281-322.

[7] S. Takakusagi, W.-J. Chun, H. Uehara, K. Asakura, Y. Iwasawa: *Top. Catal.* **2013**, *56*, 1477-1487.

[8] M. Shirai, K. Asakura, Y. Iwasawa,. *Chem. Lett.* **1992**, 1037-1040.

[9] K. Asakura, W.J. Chun, M. Shirai, K. Tomishige, Y. Iwasawa, *J. Phys. Chem. B* **1997,** *101*, 5549-5556.

[10] Y. Tanizawa, T. Shido, W.J. Chun, K. Asakura, M. Nomura, Y. Iwasawa, *J. Phys. Chem. B* **2003,** *107*, 12917-12929.

[11] Y. Tanizawa, W.J. Chun, T. Shido, K. Asakura, Y. Iwasawa, *J. Synchrotron Rad.* **2001,** *8*, 508-510.

[12] M. Shirai, T. Inoue, H. Onishi, K. Asakura, Y. Iwasawa, *J. Catal.* **1994,** *145*, 159-165.

[13] K. Asakura, W.J. Chun, Y. Iwasawa, *Jpn. J. Appl. Phys.* **1999,** *38-41*, 40-43.

[14] W.-J. Chun, Y. Koike, K. Ijima, K. Fujikawa, H. Ashima, M. Nomura, Y. Iwasawa, K. Asakura, *Chem. Phys. Lett.* **2007,** *433*, 345-349.

[15] S. Takakusagi, H. Nojima, H. Ariga, H. Uehara, K. Miyazaki, W.-J. Chun, Y. Iwasawa, K. Asakura: *Phys. Chem. Chem. Phys.* **2013**, *15*, 14080-14088.

[16] K. Asakura, S. Takakusagi, H. Ariga, W.-J. Chun, S. Suzuki, Y. Koike, H. Uehara, K. Miyazaki, Y. Iwasawa: *Faraday Discuss.* **2013**, *162*, 165-177.

[17] S. Takakusagi, A. Kunimoto, N. Sirisit, H. Uehara, T. Ohba, Y. Uemura, T. Wada, H. Ariga, W.-J. Chun, Y. Iwasawa, K. Asakura: *J. Phys. Chem. C* 2016, **120**, 15785-15791.

[18] E.T. Baxter, M.-A. Ha, A.C. Cass, A.N. Alexandrova, S.L. Anderson, *ACS Catal.* **2017***, 7,* 3322-3335.

[19] S. Bonanni, K. Aït-Mansour, W. Harbich, H. Brune, *J. Am. Chem. Soc.* **2014***, 136,* 8702−8707.

[20] F.S. Roberts, M.D. Kane, E.T. Baxter, S.L. Anderson, *Phys. Chem. Chem. Phys.* **2014**, *16*, 26443-26457.

[21] Y. Watanabe, X. Wu, H. Hirata, N. Isomura, *Catal. Sci. Technol*. **2011**, *1*, 1490-1495.

[22] W.E. Kaden, Wi.A. Kunkel, M.D. Kane, F.S. Roberts, S.L. Anderson, *J. Am. Chem. Soc.* **2010**, *132*, 13097-13099.

[23] D.P. Woodruff, *Rep. Progr. Phys.*, **2005**, *68*, 743-798.

[24] D.P. Woodruff, *Prog. Surf. Sci.,* **1998***, 57,* 1-60.

[25] J. Zegenhagen, *Surf. Sci. Rep., **1993**, 18, 1*99-271.

[26] H. Daimon, *J. Phys. Soc. Jpn.*, **2018**, *87*, 061001.

[27] D.P. Woodruff, *Surf. Sci. Rep.,* **2007,** *62*, 1-38.

[28] C.S. Fadley, Y. Chen, R.E. Couch, H, Daimon, R. Denecke, J.D. Denlinger, H. Galloway, Z. Hussaint, A.P. Kaduwela, Y.J. Kim, P.M. Len, J. Liesegang, J. Menchero, J. Morais, J. Palomares, S.D. Ruebush, E. Rosenberg, M.B. Salmeron, R. Scalettar, W. Schattke, R. Singh, S. Thevuthasan, E.D. Tober, M.A. Van Hove, Z. Wang, R.X. Ynzunz, *Prog. Surf. Sci.,* **1997,** *54*, 341-386.

[29] a) C.L. Pang, R. Lindsay, G. Thornton, *Chem. Soc. Rev*. 2013, **113**, 3887-3948 ; b) U. Diebold, *Surf. Sci. Rep.* **2013**, *48*, 53-229.

[30] D.A. Chen, M.C. Bartelt, R.Q. Hwang, K.F. McCarty, *Surf. Sci.* **2000**, *450*, 78-97.

[31] A.L. Ankudinov, B. Ravel, J.J. Rehr, S.D. Conradson, *Phys. Rev. B* **1998**, *58*, 7565-7576.

[32] K. Ding, J. Lia and Y. Zhang, *J. Mol. Struct.: THEOCHEM* **2005**, *728*, 123-127.

[33] W.-J. Chun, K. Miyazaki, N. Watanabe, Y. Koike, S. Takakusagi, K. Fujikawa, M. Nomura, Y. Iwasawa and K. Asakura: *J. Phys. Chem. C* **2013**,*117*, 252-257.

[34] Y. Koike, K. Ijima, W.-J.Chun, H. Ashima, T. Yamamoto, K. Fujikawa, S. Suzuki, Y. Iwasawa, M. Nomura, K. Asakura, *Chem. Phys. Lett*. **2006**, *421*, 27-30.

[35] Y. Koike, K. Fujikawa, S. Suzuki, W.-J. Chun, K. Ijima, M. Nomura, Y. Iwasawa, K. Asakura, *J. Phys. Chem. C* **2008**, *112*, 4667-4675.

[36] K. Fujikawa, S. Suzuki, Y. Koike, W.-J. Chun, K. Asakura: *Surf. Sci.* **2006**, *600*, L117-L121.

[37] P.L. Cao, D.E. Ellis, V.P. Dravid, *J.Mater. Res*. **1999**, *14*, 3684-3689.

[38] J.B. Park, S.F. Conner, D.A. Chen, *J. Phys. Chem. C* **2008**, *112*, 5490-5500.

[39] *CRC Handbook of Chemistry and Physics*, *Internet Version 2005*, (Eds.: E.R. Lide) <http://www.hbcpnetbase.com>, CRC Press, Boca Raton, FL **2005**.

[40] H. Toulhoat, P. Raybaud, S. Kasztelan, G. Kresse, J. Hafner, *Catal. Today* **1999,** *50*, 629-636.

[41] Y. Nagano, *Therm. Anal. Calorim.* **2002,** *69*, 831-839.

[42] *An Introduction to Ultrathin Organic Films: From Langmuir-Blodgett to Self-Assembly*, (Eds.: A. Ulman), Academic Press, San Diego, **1991**, pp 279-296.

PERSONAL ACCOUNT

Precise control of the 3D structure of highly dispersed metal species such as metal complexes and subnano-clusters attached to an oxide surface has been important for the development of high-performance heterogeneous catalysts. We have developed the “premodified surface method” to obtain an ultra-highly dispersed metal species (single metal dispersion) on an oxide single-crystal surface and explored the possibility of fine tuning and orientation control of the surface metal 3D structures.

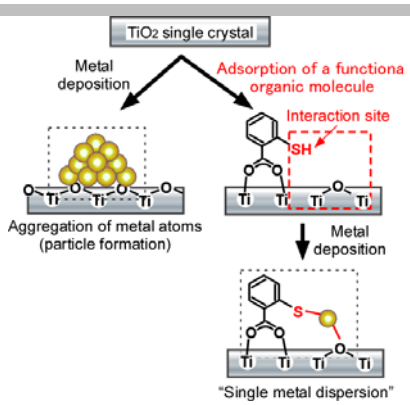

Satoru Takakusagi, Yasuhiro Iwasawa, Kiyotaka Asakura*

Page No. – Page No.

Title

Premodified Surface Method to Obtain Ultra-highly Dispersed Metals and their 3D Structure Control on an Oxide Single-crystal Surface

Table 1. Curve fitting results for Pt/*o*-MBA/TiO_2(110) data obtained at three different polarization directions.[a] N^*, r, ΔE, σ are the effective coordination number, bond distance, energy shift in the origin of the photoelectron kinetic energy and Debye-Waller factor, respectively. Reproduced with permission from Ref. 17. Copyright (2016) American Chemical Society.

Orientation	Bond	N^*	r / nm	ΔE / eV	σ / 10^{-5} nm	*R factor*
E // [001]	Pt-S	1.1±0.2	0.230±0.002	6±2	0.008±0.002	1.4 %
	Pt-Pt	1.8±0.4	0.267±0.002	0±2	0.007±0.001	
E // $[1\bar{1}0]$	Pt-S	1.2±0.2	0.229±0.002	(6)	(0.008)	1.1 %
	Pt-Pt	1.7±0.3	0.268±0.002	(0)	(0.007)	
E // [110]	Pt-S	1.2±0.2	0.229±0.003	(6)	(0.008)	5.1 %
	Pt-Pt	1.5±0.3	0.266±0.003	(0)	(0.007)	

[a]Parentheses indicate those values fixed during the fitting procedure.

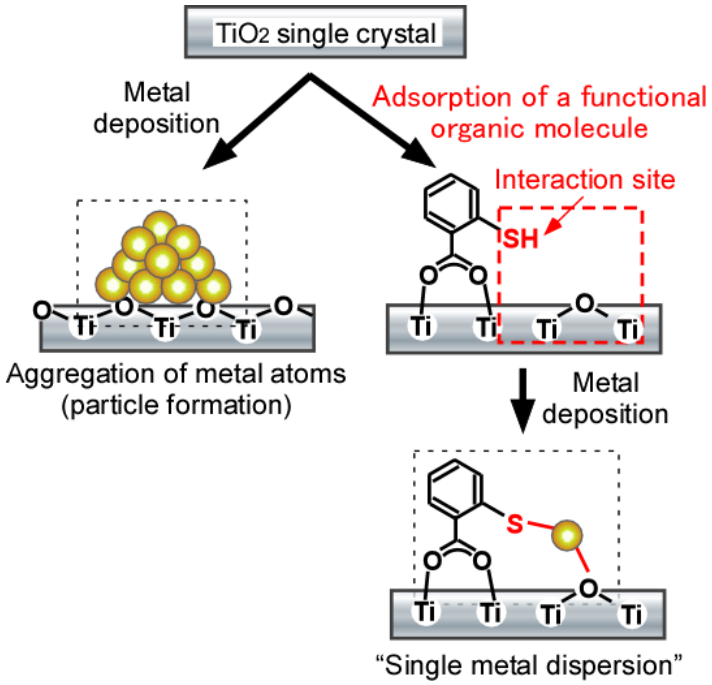

Figure 1. Surface premodification by a functional organic molecule to obtain an ultra-highly dispersed metal (single metal dispersion) on an oxide single-crystal surface.

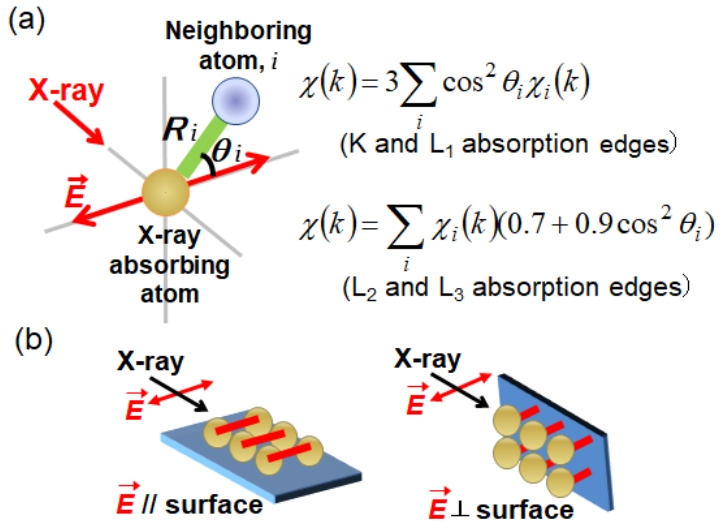

Figure 2. (a) Polarization dependence of XAFS oscillation $\chi(k)$. $\chi_i(k)$ is the XAFS oscillation originated from the bond R_i. (b) PTRF-XAFS measurements by sample rotation.

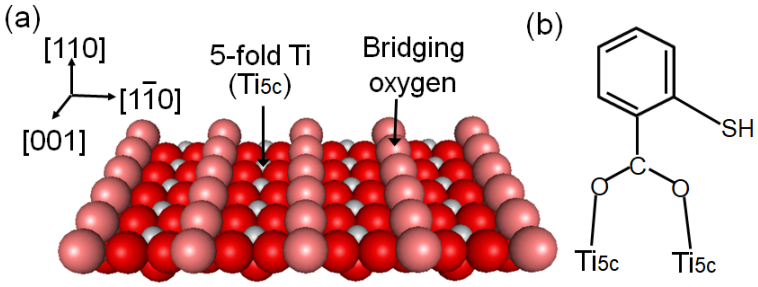

Figure 3. (a) Structure model of the TiO_2(110) surface. (b) Adsorbed structure of *o*-MBA on TiO_2(110). Reprinted with permission from Ref. 17. Copyright (2016) American Chemical Society.

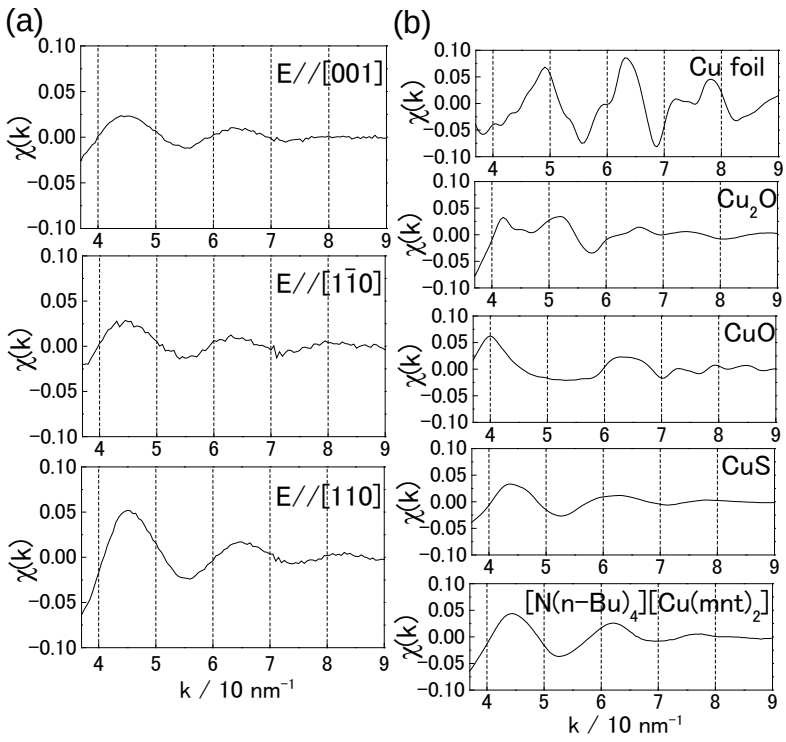

Figure 4. (a) Cu K-edge PTRF-XAFS spectra of Cu/*o*-MBA/TiO_2(110). (b) Cu K-edge XAFS spectra of reference compounds. Reproduced from Ref. [15] with permission of The Royal Society of Chemistry.

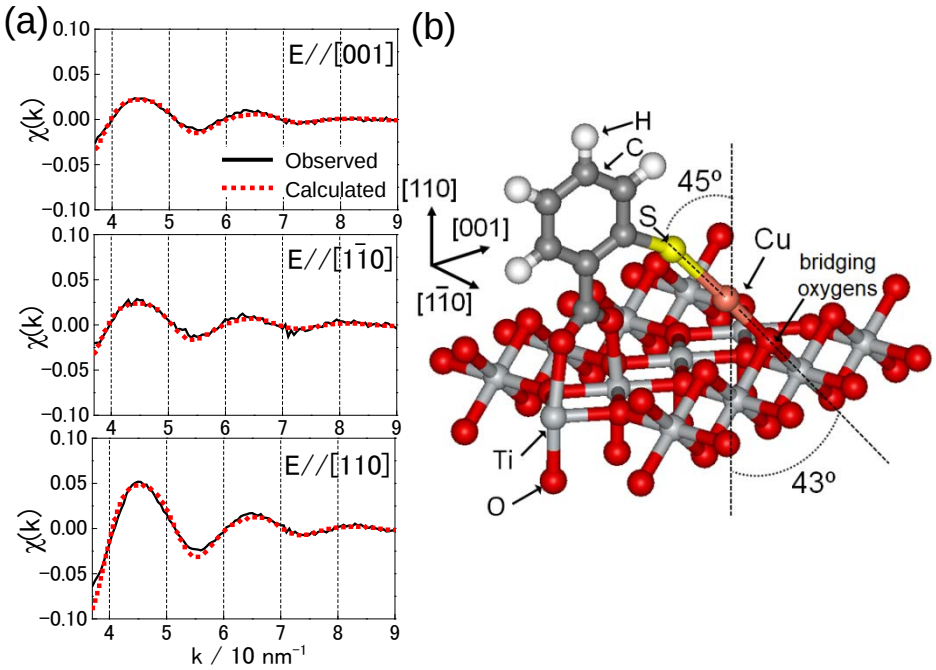

Figure 5. (a) Observed (black solid lines) and calculated (red dotted lines) PTRF-XAFS spectra for Cu/*o*-MBA/TiO_2(110), respectively. The 3D model structure shown in (b) was used to calculate the theoretical $\chi(k)$ in (a). Reproduced from Ref. [15] with permission of The Royal Society of Chemistry.

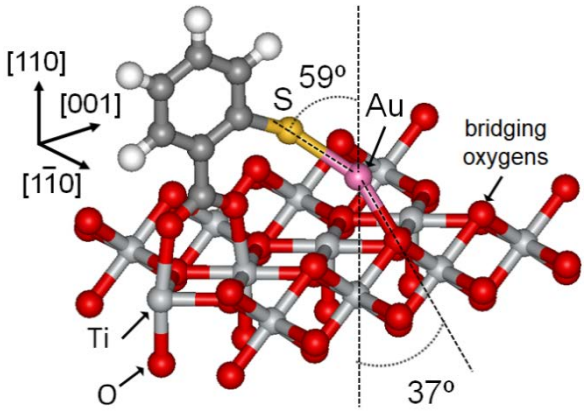

Figure 6. 3D model structure for Au/*o*-MBA/TiO_2(110). Reproduced from Ref. [16] with permission of The Royal Society of Chemistry.

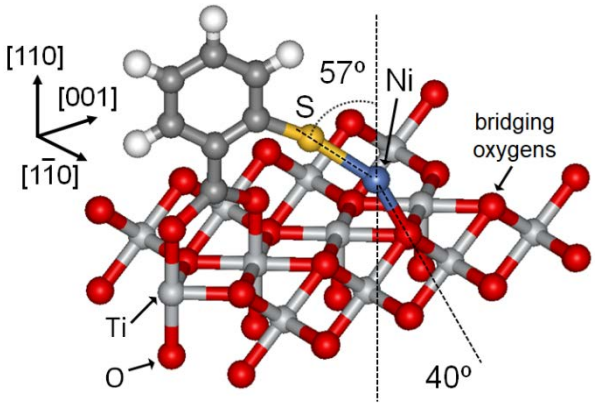

Figure 7. 3D model structure for Ni/*o*-MBA/TiO_2(110). Reprinted with permission from Ref. 17. Copyright (2016) American Chemical Society.

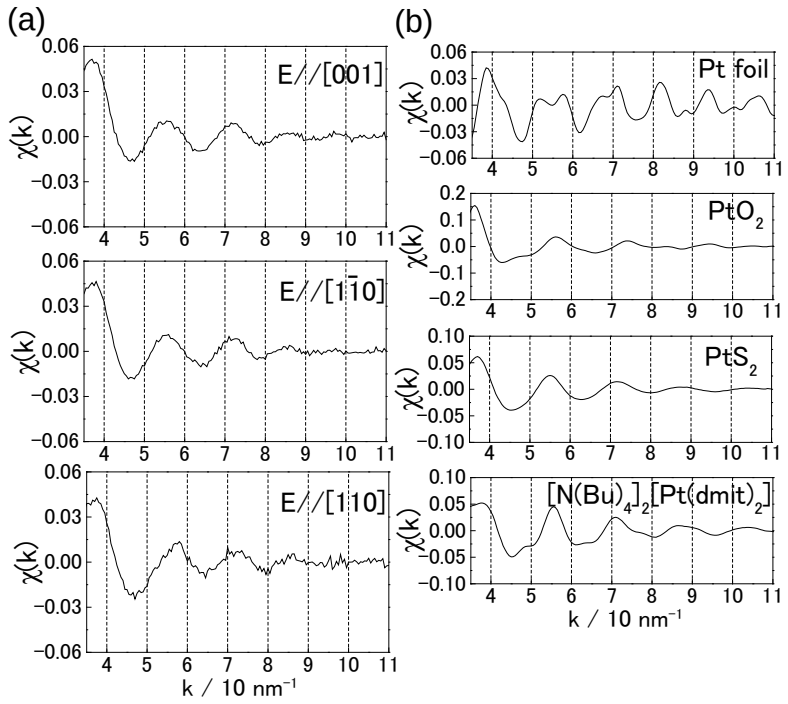

Figure 8. (a) Pt L_3-edge PTRF-XAFS spectra of Pt/*o*-MBA/TiO_2(110). (b) Pt L_3-edge XAFS spectra of reference compounds. Reprinted with permission from Ref. 17. Copyright (2016) American Chemical Society.

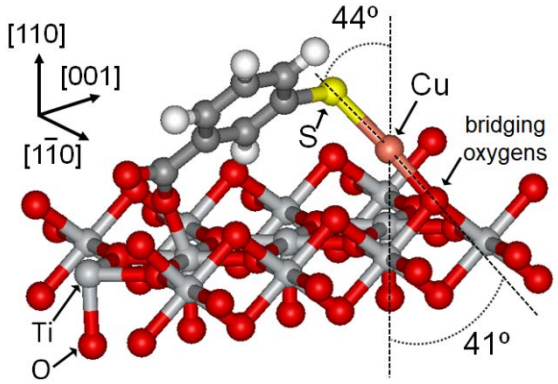

Figure 9. 3D model structure for Cu/*m*-MBA/TiO_2(110). Reproduced from Ref. [15] with permission of The Royal Society of Chemistry.

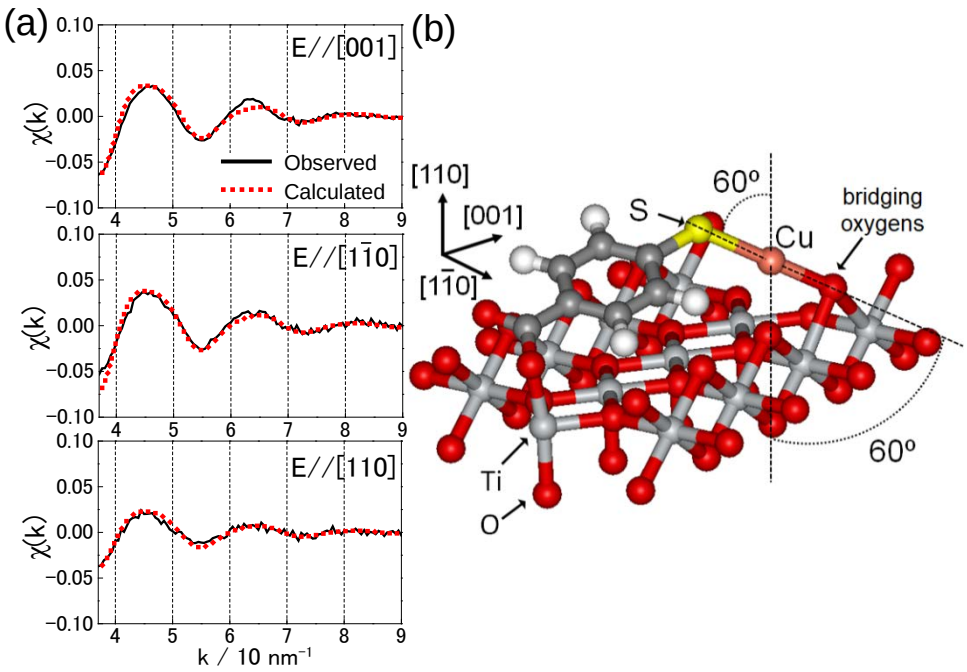

Figure 10. (a) Observed (black solid lines) and calculated (red dotted lines) PTRF-XAFS spectra for Cu/*p*-MBA/TiO_2(110). The 3D model structure shown in (b) was used to calculate the theoretical $\chi(k)$ in (a). Reproduced from Ref. [15] with permission of The Royal Society of Chemistry